Reference: *Biol. Bull.* **205:** 261–275. (December 2003)

Dynamic Mechanical Properties of Body-Wall Dermis in Various Mechanical States and Their Implications for the Behavior of Sea Cucumbers

TATSUO MOTOKAWA* AND AKIFUMI TSUCHI

Department of Biological Sciences, Graduate School of Bioscience and Biotechnology, Tokyo Institute of Technology, Meguro, Tokyo, 152-8551 Japan

Abstract. The dermis of the sea cucumber body wall is a typical catch connective tissue that rapidly changes its mechanical properties in response to various stimuli. Dynamic mechanical properties were measured in stiff, standard, and soft states of the sea cucumber *Actinopyga mauritiana*. Sinusoidal deformations were applied, either at a constant frequency of 0.1 Hz with varying maximum strain of 2%–20% or at a fixed maximum strain of 1.8% with varying frequency of 0.0005–50 Hz. The dermis showed viscoelasticity with both strain and strain-rate dependence. The dermis in the standard state showed a J-shaped stress-strain curve with a stiffness of 1 MPa and a dissipation ratio of 60%; the curve of the stiff dermis was linear with high stiffness (3 MPa) and a low dissipation ratio (30%). Soft dermis showed a J-shaped curve with low stiffness (0.3 MPa) and a high dissipation ratio (80%). The strain-induced softening was observed in the soft state. Stiff samples had a higher storage modulus and a lower tangent δ than soft ones, implying a larger contribution of the elastic component in the stiff state. A simple molecular model was proposed that accounted for the mechanical behavior of the dermis. The model suggested that stiffening stimulation increased intermolecular bonds, whereas softening stimulation affected intra-molecular bonds. The adaptive significance of each mechanical state in the behavior of sea cucumbers is discussed.

Introduction

Echinoderms have collagenous connective tissues that can alter their mechanical properties rapidly under nervous control (Motokawa, 1984a; Wilkie, 1996). Connective tissue with such mutability is called catch connective tissue or mutable connective tissue. The mutability has been attributed to the changes in the mechanical properties of the extracellular materials in the tissue (Motokawa, 1984a; Wilkie, 2002; Tipper *et al.*, 2003). The dermis in the body wall of sea cucumbers is a favored material for studies of connective tissue catch because of its large size. The mechanical properties of the dermis have been described by various mechanical methods such as creep tests (Motokawa, 1981; Eylers, 1982), stress-strain tests (Motokawa, 1982), stress-relaxation tests (Motokawa, 1984b; Greenberg and Eylers, 1984), tensile tests (Motokawa, 1982), and dynamic tests (Shibayama *et al.*, 1994; Szulgit and Shadwick, 2000). These studies revealed the viscoelastic nature of the dermis. They drew, however, contradictory conclusions about which component, elastic or viscous, changed during alterations in mechanical properties. Motokawa (1984b) concluded from the results of creep tests and stress-relaxation tests that the changes in the mechanical properties mainly occurred in the viscous component, whereas Szulgit and Shadwick (2000) concluded that it was the elastic component that changed. The former used a fixed strain and the latter a fixed strain and strain rate. The apparently contradictory conclusions of these two studies are not surprising, because viscoelastic materials exhibit different properties when tested under different conditions of strain and strain rate (Wainwright *et al.*, 1976). Therefore, description of the mechanical properties of viscoelastic materials is not satisfactory in a limited range of strain and strain rate. The present study was undertaken to describe the dynamic mechanical properties of the holothurian dermis under wide ranges of both strain and strain rate. The information obtained establishes a basis for understanding the mechanism of connective tissue catch and how sea cucumbers adapt to

Received 12 May 2003; accepted 5 September 2003.

* To whom correspondence should be addressed. E-mail: tmotokaw@bio.titech.ac.jp

various mechanical environments by changing the mechanical properties of the dermis.

Materials and Methods

Tissue samples

Specimens of the aspidochirotid sea cucumber *Actinopyga mauritiana* (Quay and Gaimard) were collected from the lagoon in front of Sesoko Marine Science Center, University of the Ryukyus, Okinawa. They were shipped to Tokyo Institute of Technology and kept in an aquarium in our laboratory. This sea cucumber has a thick body wall (about 1–1.5 cm). The connective tissue dermis occupies most of the thickness. The outer side of the dermis is covered with a thin epidermis, and the inner side is lined with body wall muscles. Unlike some dendrochirotid species such as *Cucumaria frondosa*, the dermis of this aspidochirotid sea cucumber looks uniform, showing no differentiation into layers. A dermis sample was dissected from the lateral interambulacrum of the body wall. Both the epidermis and muscles were removed and the middle portion of the dermis was cut out for experiments. The dimensions of the samples were measured with a caliper to a precision of 0.05 mm. The mean length of the samples from oral to aboral end was 2.3 mm (±0.89 mm SD; $n = 79$), and the mean cross-sectional area was 5.4 mm^2 (±1.9 mm^2 SD; $n = 79$). The samples were rested in artificial seawater of normal composition (ASW) for 17–24 h before being subjected to mechanical tests. The temperature of the seawater was 18–25 °C, which roughly corresponded to the temperature of the water from which the sea cucumbers were collected. Mechanical tests were performed at a constant temperature of 20 °C.

Samples that were rested in ASW for 17–24 h and tested in ASW are described here as being in a standard state. Soft-state samples were prepared by removal of calcium ions (Hayashi and Motokawa, 1986); they were rested in calcium-free artificial seawater (CaFASW) and tested in CaFASW. Stiff-state samples are those that were tested in ASW without a resting period. Rough physical handling makes the dermis stiffen reversibly (Motokawa, 1984c). Soon after the dissection, the dermis experienced quite rough physical handling, so these are termed the physically stimulated samples. This state probably corresponds to the state the sea cucumbers are in after being stimulated physically. Two other kinds of stimulation were employed to invoke the stiff state (possibly through stimulating the stiffening mechanism *in vivo*)—chemical stimulation by the neurotransmitter acetylcholine (ACh) (Motokawa, 1987) and chemical stimulation using artificial seawater with an elevated potassium concentration (KASW). The latter likely stimulates a cellular mechanism that controls stiffness, such as nerves, through depolarization (Motokawa, 1981).

The samples for chemical stimulation were rested for 17–24 h in ASW, and chemicals were applied 20 min before the mechanical testing. The composition of ASW was as follows (in mmol/l): NaCl, 433.7; KCl, 10.0; $CaCl_2$, 10.1; $MgCl_2$, 52.5; $NaHCO_3$, 2.5. In KASW, the concentration of potassium was raised to 100 mmol/l, and CaFASW contained 5 mmol/l EGTA (ethylene glycol bis(β-aminoethyl-ether)-*N*, *N*, *N*′, *N*′-tetraacetic acid). In both cases, the sodium concentration was adjusted to keep the osmotic concentration constant. ACh concentration was 10^{-4} mol/l in ASW. The pH of all the solutions was adjusted to 8.2.

Experimental apparatus

A dermis sample was subject to forced vibrations using sinusoidal displacements. The sample was stretched and compressed cyclically, and the resulting forces were recorded. The experimental apparatus (Fig. 1) included a vibrator (511-A, EMIC, Japan) driven by sinusoidal currents that were generated by a function generator (SG-4101, Iwatsu, Japan). The force developed in the dermis was measured by a micro load cell (LTS-200GA, Kyowa, Japan). The compliance of the load cell was 0.3 μm/g, which contributed at most 4% to the measured value of strain in the present experiments. The deformation of the dermis was monitored by an eddy-current displacement sensor (502-F, EMIC, Japan). Force signals were amplified by a strain amplifier (DPM-602A, Kyowa, Japan). Both force and displacement signals were displayed on an oscilloscope and simultaneously recorded by a computer through a data-acquisition unit (Lab Stack, Keisoku Giken, Japan). The dermis sample was glued with cyanoacrylate glue to the holders, one attached to the vibrator and the other to the load

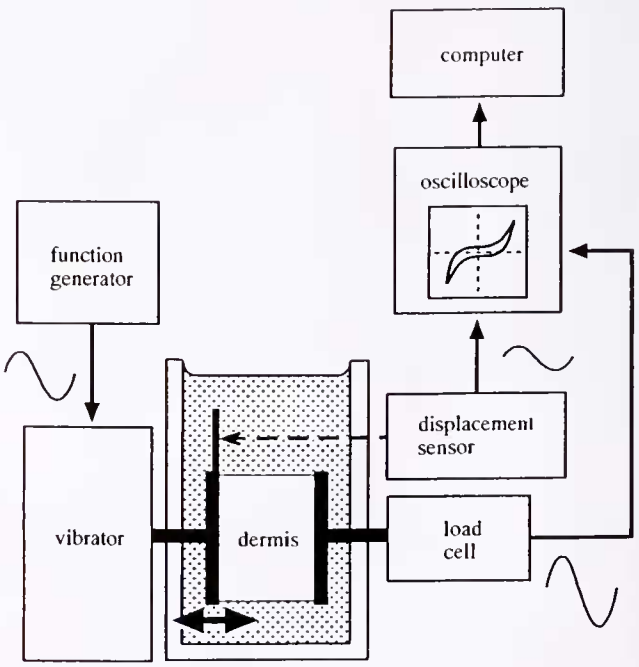

Figure 1. Schematic of the experimental apparatus for dynamic tests.

cell, and an experimental solution was introduced to the trough. The sample was usually rested for 20 min in the trough; however, the physically stimulated sample was tested immediately. The trough was water-jacketed to keep the temperature constant at 20 °C.

We performed two series of experiments. In the constant-frequency experiments, the frequency of vibration was kept constant at 0.1 Hz and the maximum strain in a cycle was varied between 2% and 20%. A frequency of 0.1 Hz was chosen because the differences in the mechanical properties of the three states were most prominent at this frequency (see Results). In the constant-maximum-strain experiments, the maximum strain in a cycle was kept at 1.8% and the frequency was varied between 0.0005 and 50 Hz. A maximum strain of 1.8% was chosen because the dermis behaved as a linear viscoelastic material at this strain (see Results).

The samples were preconditioned by applying oscillations for 10 min prior to the test; the amplitude and frequency were the same as those in the test. A steady-state response was reached by the preconditioning.

Constant-frequency experiment

In experiments that examined the effects of strain, a dermis sample was subjected to successive oscillatory tests with different levels of maximum strain. The hysteresis loop of the stress-strain relationship showed almost point symmetry. The point of symmetry was brought to the origin of the coordinates by adjusting the length of the sample. Data were then collected, and a typical hysteresis loop was generated for that maximum strain. When the data acquisition was finished at a certain maximum strain, the maximum strain in an oscillatory cycle was increased by about 4% (range 2%–7%), the sample was preconditioned, and data were collected with the new maximum strain.

Strain (ε) was defined as the length change divided by the original length of the sample, and stress (σ) as the force divided by the cross-sectional area at the original length. When stress was plotted against strain, a closed hysteresis loop was obtained (Fig. 2). Because the dermis behaved quite similarly in tension and in compression, the values given in this paper are the averages of the absolute values at equal strains in tension and in compression. The maximum strain imposed in a loop was denoted as the maximum strain (ε_{max}), and the maximum stress observed in a loop was denoted as the maximum stress (σ_{max}). A quarter of the loop had the shape of the letter "J" with a flat "toe" region and a more vertical "pole" region. We introduced an index (the J index) to quantify the degree of concavity of the stress-strain curves in the loading and unloading phases in tensile strain. We defined the J index as the area enclosed by the stress-strain curve and the line connecting the peak point with the intersecting point at 0 strain in the curve, divided by the area of a right triangle whose hypotenuse was the same line as before, one side was a horizontal extending from the intersecting point, and the other side was a vertical extending from the peak point (Fig. 2 inset). The J index was equivalent to the difference between the energy fed into the specimen and the deformation energy of an elastic body with a linear stress-strain curve; the J index is thus a measure of how concave the stress-strain curve was. The J index was defined as 0 when the curve was convex. The stiffness was defined as the slope between the two peaks of a hysteresis loop. The deformation energy (E_t) was defined as the hatched area in Figure 2. It corresponds to the energy required to deform the dermis of a unit volume for one cycle. In each cycle of deformation, the deformation energy is partly conserved and reused as elastic recoil to restore the geometry of the sample; the rest is dissipated and lost, primarily as thermal energy. The energy dissipated (E_d) corresponds to the area enclosed by the hysteresis loop. The dissipation ratio D was defined as $D = E_d/E_t$ and was expressed as a percentage.

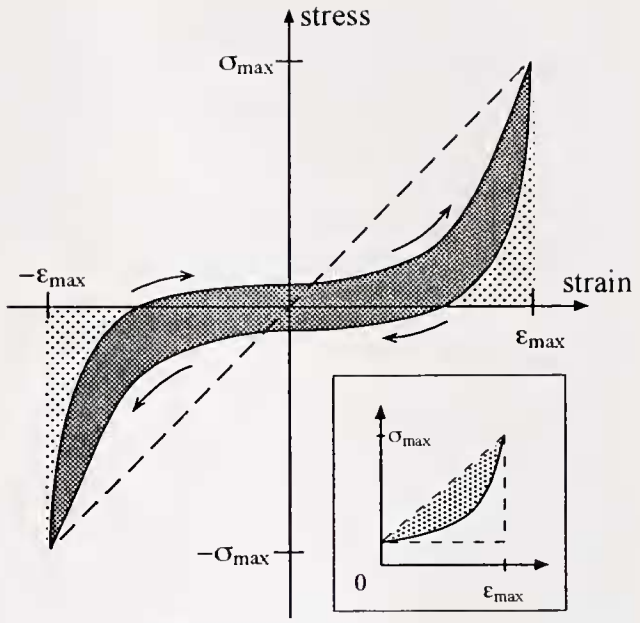

Figure 2. Schematic of a hysteresis loop of the dermis in standard state under a sinusoidal deformation of 10% maximum strain at 0.1 Hz. The loop showed clockwise rotation (arrows). The stiffness was defined as the slope of the dotted line. The darker hatched area represents the dissipated energy, the lighter hatched areas the conserved energy, and the total hatched area the deformation energy. The inset shows how the J index was measured: it was the percent ratio of the hatched area to the area of the triangle shown by dotted lines.

The limit strain was estimated as the average of the smallest maximum strain that caused the strain-induced softening and a maximum strain one step smaller (where strain-induced softening was not observed).

Reversibility of the response was determined by successive mechanical tests using the same sample. The sample in the stiff state caused by physical stimulation was tested, then rested for 22 h and tested again. In the chemically

stimulated stiff samples, the preparations were first tested in ASW and then treated with stimulation media for 20 min before the second mechanical tests. Samples were washed thoroughly in ASW for 24 h, and the third mechanical test was performed.

We also determined whether softening induced by stretching the samples in CaFASW beyond the limit strain was recoverable when the maximum strain was reduced to less than the limit strain. The sample was tested at $\varepsilon_{max} = 2\%$ in CaFASW. Then oscillations of ε_{max} of about 30% were given for 10 min, and the sample was tested again at $\varepsilon_{max} = 2\%$.

Constant-maximum-strain experiment

In this experiment, the maximum strain was kept constant at 1.8% and the frequency was varied in a dermis sample. A sample was tested first at 0.1 Hz. Then the test frequency was either increased stepwise to 0.5, 1, 5, 10, and 50 Hz or decreased to 0.05, 0.01, 0.005, 0.001, and 0.0005 Hz. The data from 10 cycles at each frequency were averaged in all experiments except at the lowest two frequencies, where data for two cycles were averaged.

In a viscoelastic material, stress and strain are not in phase—rather, strain lags behind stress by a phase angle δ. For a linear viscoelastic material, the complex modulus E^*, the storage modulus E', and the loss modulus E'' are defined as follows (Oka, 1974).

$$E^* = \sigma/\varepsilon = E' + iE''$$

$$E' = |E^*| \cos \delta$$

$$E'' = |E^*| \sin \delta$$

$$\tan \delta = E''/E'$$

The complex modulus represents the conventional "stiffness." The storage modulus is equivalent to the elastic modulus in phase with the stress and is a measure of the energy elastically stored in each cycle. The loss modulus is the out-of-phase component and is a measure of the energy dissipated. Tangent δ is the ratio of the energy lost to the energy stored.

The soft state was induced by a vibration of 0.1 Hz with ±20% maximum strain applied for 30 min in CaFASW. Such a treatment caused strain-induced softening (see Results). The softened sample was subsequently tested in CaFASW.

Results

Constant-frequency experiments

Hysteresis loop at maximum strain = 10% and frequency = 0.1 Hz. When stress was plotted against strain, a closed hysteresis loop of clockwise rotation was generated. The loop could be divided into four phases: a tensile phase in which the dermis was gradually stretched, a tension-unloading phase in which the tensile strain decreased, a compressing phase in which the dermis was gradually compressed, and a compression-unloading phase in which the compressive strain decreased.

The hysteresis loop of a sample in the standard state at 10% maximum strain is shown in Figure 3a. When stretched from zero strain, the dermis could be deformed quite easily; thus the slope of the curve was flat at first, corresponding to the toe region of the J. When strain exceeded about 5%, the slope became progressively steeper; thus the tensile stress-strain relation followed a typical J-shaped curve (Wainwright *et al.*, 1976). The J index averaged 43% (±9.1% SD, $n = 17$). After the tensile stress peaked, the unloading phase started and stress decreased rapidly. The slope was steeper than that in the loading phase at each strain. As the strain progressively decreased, the slope declined and the curve became almost flat. The J index of the unloading phase averaged 71% (±13% SD, $n = 17$), much greater than that of the loading phase (significant difference by paired t test, $P < 0.01$). In the loading and unloading phases of the compression half of the cycle, the curve followed almost the same course as that of the tensile half with the sign of stress and strain reversed. Thus the dermis behaved similarly in tension and compression. The four phases of the hysteresis loop all exhibited a J shape, and the whole loop showed approximate point symmetry.

The loops of stiff samples differed from those of samples in the standard state both in shape and in the stress developed (Fig. 3b, c, d). The J shape became less prominent: the toe region became short (restricted to strains under 2%–4%) and was not flat but had a steep slope so that there was only a small kink between toe and pole. Thus each phase of the hysteresis loop in stiff samples was rather straight, which made the J index small. The J indices of the loading phase in samples stiffened by physical stimulation, KASW stimulation, and ACh stimulation were 9.0% ± 8.2% ($n = 4$), 19% ± 11% ($n = 4$), and 26 ± 6.0 ($n = 5$), respectively (average ± SD). The average J indices were significantly smaller than that of the standard state (Scheffé test, $P < 0.01$). In stiff samples, the shape of the stress-strain curve during the unloading phase showed no great difference from that of the loading phase. The J indices during the unloading phase in samples stiffened by physical stimulation, KASW stimulation, and ACh stimulation were 14% ± 8.6% ($n = 4$), 23% ± 12% ($n = 4$), and 33 ± 8.9 ($n = 5$), respectively (average ± SD). The J index of the unloading phase in a hysteresis curve was slightly larger than that of the loading phase, but the statistical comparison of the averages showed no significant difference. In stiff samples, the maximum stress was much larger and the area enclosed by a loop was much smaller than in samples in standard state. These features implied that the stiffened dermis behaved like a stiff, resilient spring.

The hysteresis loop of soft samples was rather flat in

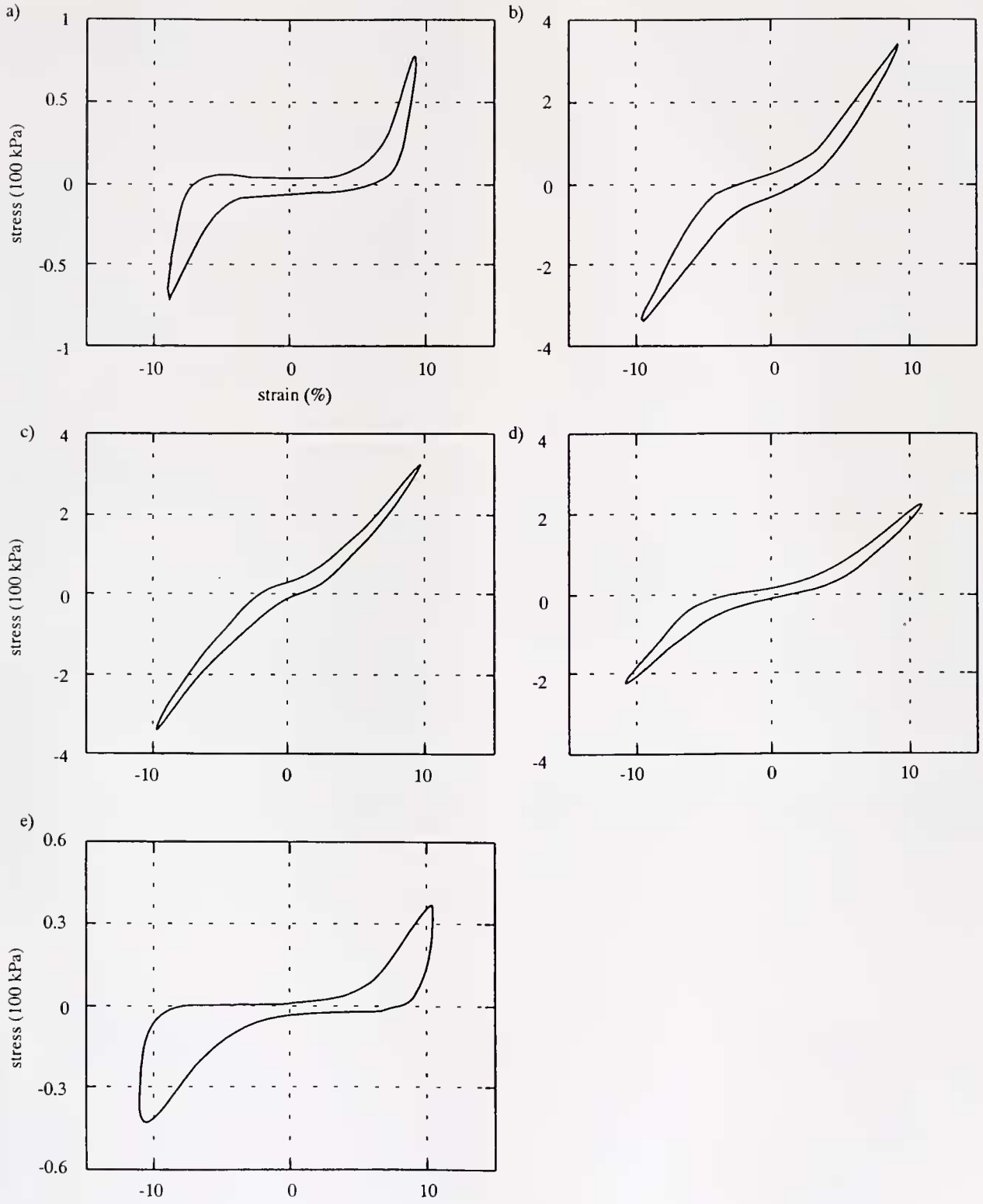

Figure 3. Typical hysteresis loops at 10% maximum strain and 0.1 Hz frequency. (a) Standard state. (b–d) Stiff state induced by physical stimulation (b), by KASW (c), and by 10^{-4} mol/l acetylcholine (d). (e) Soft state.

loading (Fig. 3e). This is because the toe region was similar, both in length (strain) and in height (stress) to that of the standard, but the pole was shorter; for example, the maximum stress was much smaller in the soft state than in the standard state. The J index in loading phase averaged 27% ± 8.9% (average ± SD, $n = 9$) which was significantly

smaller than that of the standard state (Scheffé test, $P < 0.01$). The shape of the stress-strain curve during the unloading phase showed marked differences from that of the loading phase. In the unloading phase, stress sharply decreased from the peak to give a J index as high as 86% ± 7.1% (average ± SD, $n = 9$), which was statistically different from that of the loading phase (paired t test, $P < 0.01$). This made the area enclosed by the hysteresis loop larger. These features implied that the dermis in the softened state became more compliant and less resilient.

Influence of maximum strain on the hysteresis loop. At $\varepsilon_{max} = 0.5\%–3\%$, the hysteresis loop followed a skewed ellipse regardless of the state of the samples, showing no signs of the J-shaped curve seen at larger strains. Both E^* and tan δ were constant in this strain range. Thus the dermis behaved as a linear viscoelastic material.

The maximum strain was increased stepwise by increments of 2%–4% starting from $\varepsilon_{max} = 2\%–3\%$. In standard samples, the hysteresis loops of $\varepsilon_{max} = 5\%–25\%$ were composed of prominent J curves. The peak stress became higher as ε_{max} increased (Fig. 4a). The J index increased as ε_{max} increased from 5% to 15%, and thus the stress-strain curve showed a more pronounced J shape as ε_{max} increased up to 15%. In stiff samples, the shape of the loop was quite similar for ε_{max} between 5% and 15% (Fig. 4b) with a constant J index. The maximum stress (σ_{max}) increased as ε_{max} increased. The samples detached from the holders when ε_{max} exceeded about 15%.

In soft samples, the shape of the hysteresis loop and the maximum stress both showed a marked dependence on ε_{max} (Fig. 4c). When ε_{max} was increased above 5%, σ_{max} also increased at first, but once ε_{max} exceeded a certain value (the limit strain) σ_{max} decreased as ε_{max} increased. The limit strain was 8.0%–18.2% (average = 11.2%, SD = 3.9%, $n = 6$). The hysteresis loop above the limit strain had a long toe region, which was expected from the larger J index with smaller σ_{max}. The dermis ruptured when ε_{max} exceeded 18%–26%.

The sample that experienced strain-induced softening was softer than before, even when measured at strains smaller than the limit strain. The stiffness of soft samples was measured first at $\varepsilon_{max} = 2\%$ in CaFASW; values averaged 0.24 MPa (±0.12 SD, $n = 11$). The samples were then subjected to vibrations beyond the limit strain for 10 min and tested again at 2% ε_{max}. The stiffness in the second series of tests averaged 0.010 MPa (±0.005 SD, $n = 10$), which was significantly smaller (paired t test, $P < 0.01$) than the initial values. Once strain-induced softening occurred, the decreased stiffness was apparent not only at strains over the limit strain but also for strains under the limit strain.

Stiffness, deformation energy, and dissipation ratio. Table 1 summarizes the mechanical properties of the samples in each of the three states, and Figure 5 shows the dependence of mechanical properties on the maximum strain. In standard samples, the stiffness increased 2- to 3-fold as ε_{max} increased from 2% to 5%; it remained almost constant at a value of about 1 MPa above 5% (Fig. 5a). In stiff samples, the stiffness was almost independent of ε_{max} at a value of about 3 MPa, 2.5–3.5 times greater than that of standard samples. The average stiffness values of stiff samples (regardless of the stimulation used to stiffen the sample) were significantly greater than those of standard samples ($P < 0.01$) at a maximum strain of both 3% and 5% (Table 1). There were no significant differences in stiffness among stiff samples produced by different stimuli.

The stiffness was low in the soft samples. At strains less

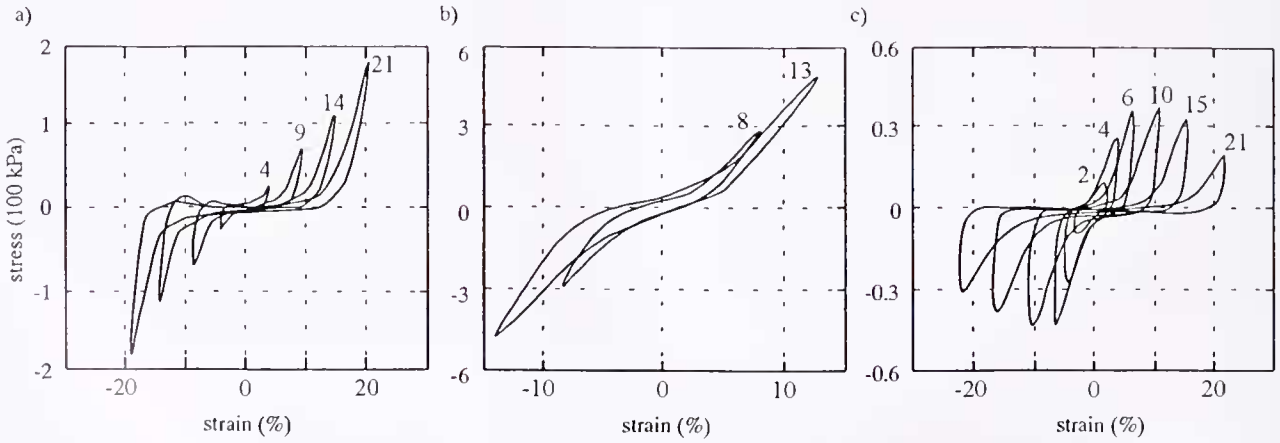

Figure 4. Typical examples of effects of maximum strain on hysteresis loops measured at 0.1 Hz: (a) standard state; (b) stiff state induced by physical stimulation; (c) soft state. The maximum strain was increased stepwise in a single sample in each state. The number above each loop is the maximum strain rounded to the nearest integer. The curves of some steps were not shown except in c. Note that in the soft state, strain-induced softening was observed, the maximum stress decreased as maximum strain increased from 10% to 21%. The limit strain was estimated as 12.7% (see text).

Table 1

Mechanical properties of sea cucumber dermis

Mechanical properties	Maximum strain 3%	10%	18%
Stiffness (MPa)			
Stiff			
physical	3.1 ± 0.37 (5)**	3.4 ± 0.61 (4)**	—
KASW	3.1 ± 0.95 (5)**	2.7 ± 0.53 (4)**	—
ACh	2.3 ± 0.60 (6)**	2.4 ± 0.85 (5)**	—
Standard	0.77 ± 0.30 (14)	1.0 ± 0.34 (17)	1.1 ± 0.32 (9)
Soft	0.28 ± 0.11 (4)	0.29 ± 0.25 (9)**	0.12 ± 0.070 (5)**
Deformation energy (kPa)			
Stiff			
physical	5.0 ± 0.85 (5)**	38 ± 6.9 (4)**	—
KASW	5.1 ± 1.1 (5)**	28 ± 9.1 (4)**	—
ACh	3.7 ± 0.61 (6)**	22 ± 7.6 (5)**	—
Standard	1.4 ± 0.53 (14)	9.4 ± 3.9 (17)	25 ± 9.8 (9)
Soft	0.48 ± 0.31 (4)	3.0 ± 2.8 (9)	3.1 ± 2.3 (5)**
Dissipation ratio (%)			
Stiff			
physical	19 ± 11 (5)**	29 ± 7.0 (4)*	—
KASW	20 ± 11 (5)**	31 ± 5.1 (4)*	—
ACh	32 ± 8.3 (6)	32 ± 11 (5)*	—
Standard	48 ± 10 (14)	59 ± 18 (17)	54 ± 12 (9)
Soft	61 ± 14 (4)	78 ± 11 (9)*	77 ± 16 (5)*

A series of data at different maximum strain were obtained from the same sample. Values are averages ± SD (n). The average is that of samples that were taken from different individuals. For 3% and 10% maximum strains, the Scheffé test was used for *post hoc* statistical analysis after the analysis of variance. An unpaired t test was used for 18% maximum strain.

* The mean is significantly different from that of the standard ($P < 0.05$).

** The mean is significantly different from that of the standard ($P < 0.01$).

— No data were obtained because the samples detached from the holders when maximum strain exceeded about 15%.

than 10%, the stiffness of soft samples was one-tenth that of the stiff state and one-third of the standard state. Because the peak stress (and thus the stiffness) decreased above the limit strain, the differences in the stiffness were more marked at $\varepsilon_{max} = 18\%$, where stiffness was one-tenth of the standard (Table 1).

Deformation energy increased with ε_{max} in all three states except for the region above the limit strain in soft samples (Fig. 5b). When compared with standard samples, stiff samples required 2–4 times more energy to deform, whereas soft samples required less energy, especially when ε_{max} exceeded the limit strain (Table 1).

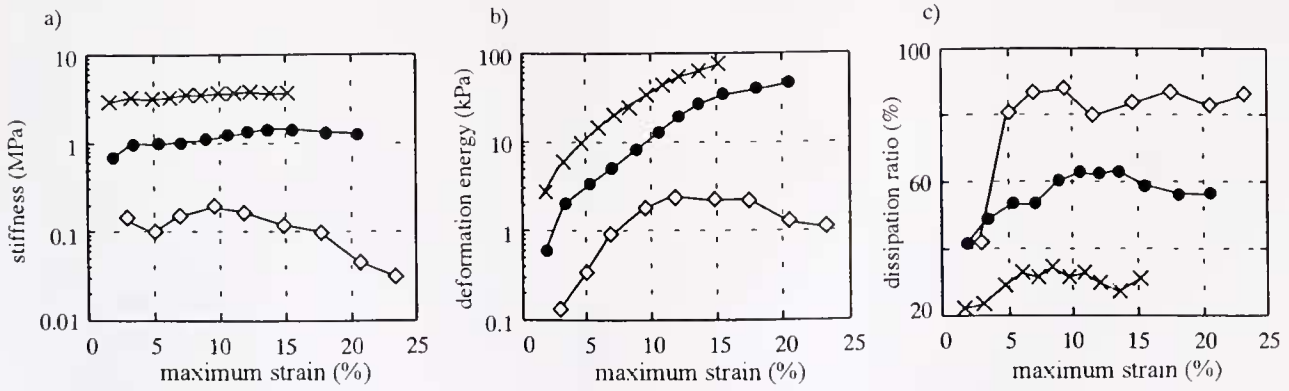

Figure 5. Effects of maximum strain on mechanical properties measured at 0.1 Hz. A typical example was chosen for each state from 5 to 6 dermis samples from different individuals: (a) stiffness; (b) deformation energy; (c) dissipation ratio. Curves with the same symbol are from the same preparation. The stiff sample (cross) was produced by physical stimulation. Filled circle, standard sample; diamond, soft sample.

The dissipation ratio increased as ε_{max} increased from 2% to 5%, but it remained almost constant for larger ε_{max} (Fig. 5c). About 60% of the deformation energy was dissipated in standard samples at $\varepsilon_{max} = 10\%$ (Table 1). The dissipation ratio was halved in stiff samples but increased to as much as 80% in soft samples. The average values at a maximum strain of 10% in the stiff and soft states were significantly different from that of the standard state ($P < 0.05$).

Reversibility of responses. Whether the stiffened dermis, which was stimulated from the standard state, resumed the standard state after removal of the stimuli was examined by successive measurements on the same sample. The stiffening response was reversible—stiffened samples resumed the standard state after resting in ASW for 1 day (Fig. 6). Although it took 2 days from the time of preparation to the completion of measurements in the chemically stimulated samples, the samples did not show any sign of decay, and the mechanical parameters in ASW after stimulation were similar to those in ASW before stimulation.

Constant-maximum-strain experiments

No increase in stress was observed during the preconditioning period, which implied that the imposed vibration of 1.8% strain did not act as a mechanical stimulus for the dermis. Stiffening of the dermis by forced vibration has been reported in other sea cucumbers but at much larger strains (Shibayama *et al.*, 1994).

The frequency dependence of E^*, E', E'', and tan δ in the standard state is given in Figure 7. The complex modulus E^* gave a sigmoid curve (Fig. 7a). E^* took a low and rather constant value of about 20 kPa at frequencies lower than 0.005 Hz. At 1 Hz and higher it showed a rather constant value of about 3 MPa. Tan δ was more or less constant in the lower frequencies with a maximum value of about 1, and for frequencies exceeding 0.01 Hz it decreased with frequency to 0.06 at 50 Hz (Fig. 7b). E' exhibited a curve similar to that of E^*, with the value for each frequency a little smaller than that of E^* (Fig. 7c). E'' also showed a sigmoid curve (Fig. 7d) with values similar to that of E' for frequencies lower than 0.01 Hz. However, E'' was about one-tenth of E' in the high-frequency range, reflecting the fact that tan δ was less than 1 at higher frequencies.

The frequency dependence of stiff and soft states is given in Figure 8. All curves of stiff states induced by different stimuli coincided well, suggesting that the three stimuli invoked an identical mechanical state.

The curve of E^* in the stiff state was different in shape and position from that in the standard state (Fig. 8a). The curve was not sigmoid. It sharply increased with frequency in the low frequency range (5×10^{-4}– 1×10^{-3} Hz); the rate of increase diminished as frequency increased, reaching a constant value of around 3 MPa. In the stiff state, E^* was higher than E^* of the standard at every frequency—by as much as two orders of magnitude at the lower frequencies. At frequencies higher than 0.5 Hz, however, the difference decreased by a factor of 2. In the soft state, E^* was different in shape and value from both those in the standard state and those in the stiff state (Fig. 8a). E^* was rather constant at a low value (about 10 kPa) for frequencies lower than 0.5 Hz but sharply increased at higher frequencies to about 1 MPa. E^* was 1/100–1/10 the value of E^* of the standard state seen in the middle frequency region (0.05–5 Hz).

Tan δ in the stiff states decreased with frequency to reach rather a constant value at 5 Hz and higher. The values were similar to those in the standard state at low frequencies (less than 0.005 Hz), but at higher frequencies tan δ was much less. In the soft state, tan δ was about 1, with a little decrease with increasing frequency in the range higher than 0.005 Hz, but a sharp drop between 0.0005 and 0.005 Hz. The values of tan δ were similar to those of the standard in the frequency range 0.005–0.05 Hz, but at in other frequencies—higher or lower—the values were much higher than those in either the standard or stiff states.

The curve of E' in the stiff state appeared on the top, that

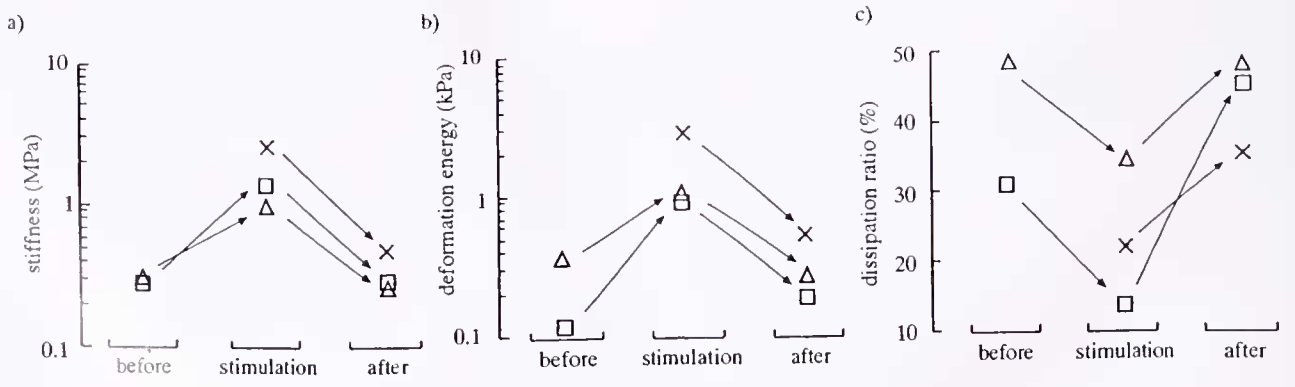

Figure 6. Reversibility of stiffening responses induced by ACh (triangle), KASW (square), and physical stimulation (cross). For chemical stimulation, measurements in ASW were made both before and after the stimulation. (a) Stiffness; (b) deformation energy; (c) dissipation ratio. Identical symbols are from the same sample.

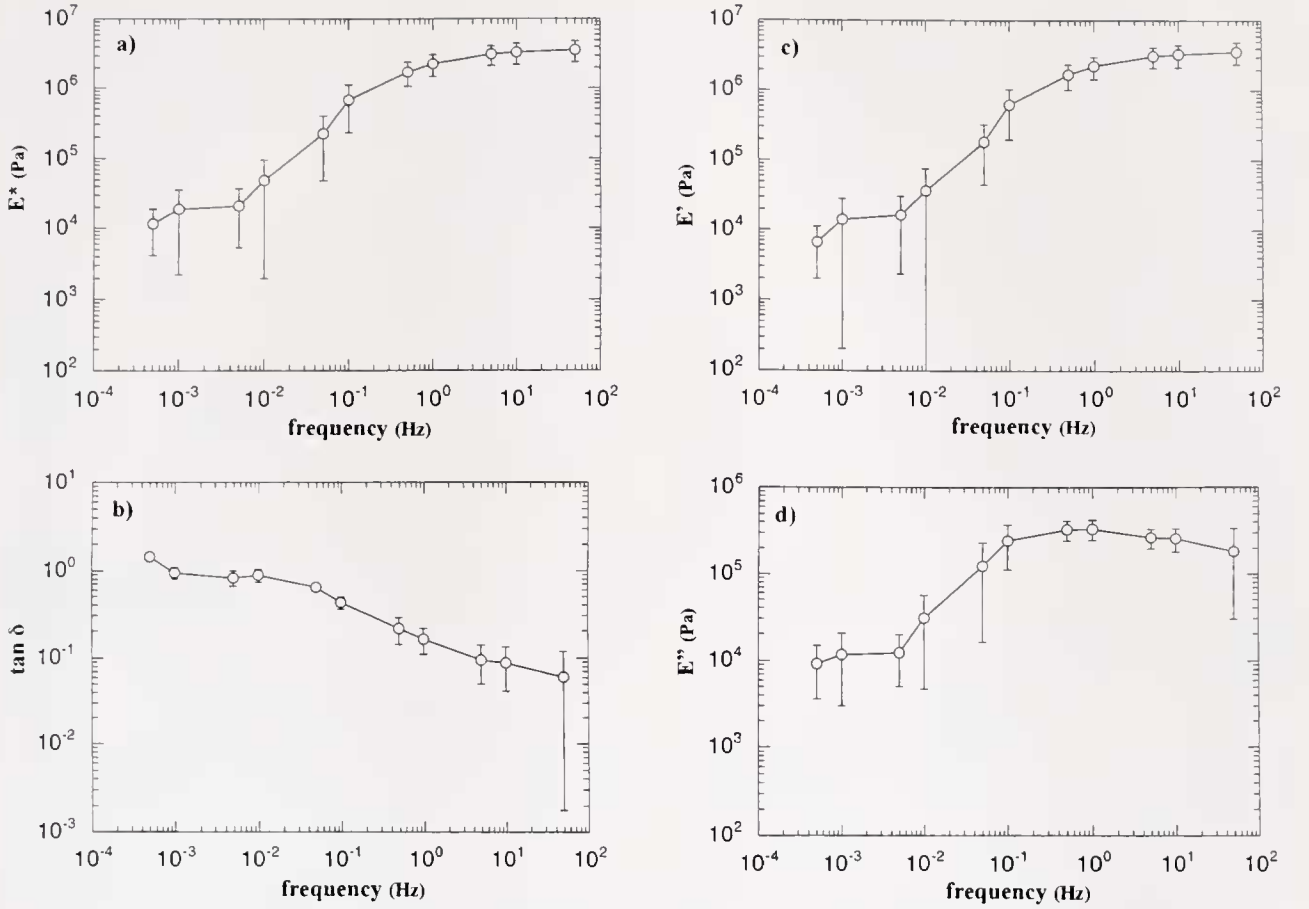

Figure 7. Frequency dependence of mechanical properties of samples in the standard state at 1.8% strain. Circles give the average of 8 samples from 4 different individuals; bars are ± SD. (a) Complex modulus E^*; (b) tangent δ; (c) storage modulus E'; (d) loss modulus E''.

in the soft state on the bottom, and that in the standard in-between (Fig. 8c). As for E^*, the difference in the values of E' became smaller with increasing frequency in the frequency range higher than 1 Hz, especially the difference between standard and stiff states. E' for the stiff state gave a curve similar to that of E^*. The curve of E' in the soft state was similar to that of E^* except at low frequencies (less than 0.005 Hz), where E' showed a sharp increase with frequency, reflecting the sharp decrease of tan δ in this frequency range.

The curve of E'' in the stiff state was rather flat with a value on the order of 100 kPa. The curve of E'' in the soft state was sigmoid, as was that in the standard. E'' increased with frequency, but plateaued above 0.1 Hz in standard state, whereas in the soft state it plateaued at a higher frequency (5 Hz). The saturated E'' value of about 200 kPa was the same in all three states (frequency range 5–50 Hz).

Comparison of curves in different states (Fig. 8) showed that both the viscous component and the elastic component changed with tissue states; the relative contributions of the two components to the changes in E^* appeared to be different at different frequencies. For example, a fairly large increase in E^* occurred at 0.005 Hz without a change in tan δ when the dermis stiffened from standard state. At this frequency, both increases in the elastic component (E') and increases in the viscous component (E'') contributed equally to the increase in E^*. At 5–50 Hz, however, a decrease in E' without changes in E'' caused a decrease in E^* when the dermis softened from the standard state.

Discussion

Strain and strain-rate dependence

The present work studied the mechanical properties of the catch connective tissue in the holothurian dermis and their changes upon stimulation. Dynamic sinusoidal strain of 0.5%–25% over a frequency range covering 5 logarithmic decades was applied and mechanical parameters were examined. This is the first description of the dynamic viscoelasticity of mutable connective tissues that systematically varied both strain and strain-rate over wide ranges. The study revealed that the viscoelastic properties of the holothurian dermis is both strain and strain-rate dependent.

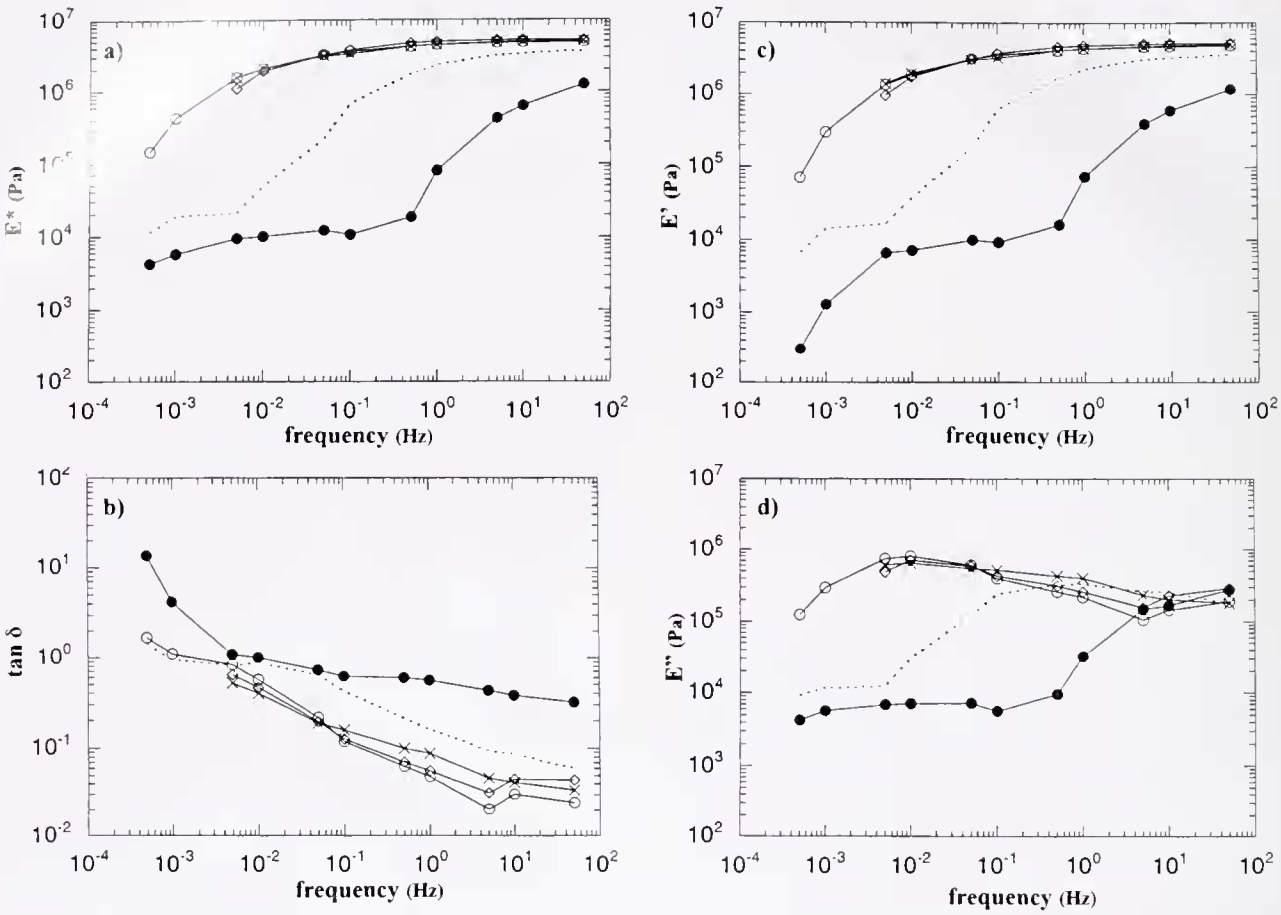

Figure 8. Frequency dependence of mechanical properties of the stiff state and of the soft state (strain 1.8%). (a) Complex modulus E^*; (b) tangent δ; (c) storage modulus E'; (d) loss modulus E''. Values are averages of 6 samples from 3 individuals. Hollow circle, stiff state (dissection); hollow diamond, stiff state (KASW); cross, stiff state (ACh); filled circle, soft state. Broken lines are the curves of the standard state.

We observed several kinds of strain dependence. The dermis behaved as a linear viscoelastic material at small strains (less than 3%), whereas it showed nonlinearity at larger strains. Two kinds of notable nonlinear strain dependence were observed. One was the J-shaped stress-strain relationship, which is a common feature of soft biological materials (Wainwright *et al.*, 1976). The J-shaped curve was apparent in the standard and soft states but not in the stiff state. The introduction of the J index enabled us to quantitatively describe the difference in the shape of the curves. The other nonlinearity, which was observed only in the soft state, was strain-induced softening—the stiffness decreased when strain exceeded the limit strain of about 10%. These nonlinear strain dependences were thus tissue-state dependent.

We obtained a modulus-frequency curve by varying the frequency. The curves of E^*, E', and E'' in the standard state were sigmoid, which clearly showed that the mechanical properties of the dermis were strain-rate dependent. The curves and thus the dependence were quite different in different tissue states. The curves of E' in stiff, standard, and soft states were different from each other, which implied that changes in elasticity accompanied the alteration in tissue states. The curves of E'' in the three states were also different, which implied that the changes in viscosity also occurred at tissue-state changes. Thus, both elasticity and viscosity changed with the changes in tissue states. The curves of tan δ for the three states gave different values at most frequencies. This clearly showed that the ratio of the contribution of the viscous component to the contribution of the elastic component changed with tissue states. The change in elasticity and the change in viscosity appeared either simultaneously or independently at a given frequency. Previous studies based on experiments with a fixed, arbitrarily selected strain rate drew contradictory conclusions on which components (elastic or viscous) mainly changed at alteration in tissue states (Motokawa, 1984b; Szulgit and Shadwick, 2000). The present study clearly showed that both components change.

Stiff state

The present study employed three different stimuli that possibly acted through stimulating the stiffening mechanism active in the intact dermis. Although the stiff state was induced by different methods, all produced almost identical parameter-frequency curves. Therefore we concluded that the same mechanical state was induced by these methods. Acetylcholine is a ubiquitous neurotransmitter that functions in the control of dermal stiffness in sea cucumbers (Motokawa, 1987; Birenheide *et al.*, 1998). The potassium-rich media very likely worked through stimulating cellular elements controlling the dermal stiffness by membrane depolarization (Motokawa, 1994). The stiffening caused by the handling at preparation likely corresponds to the dermal stiffening that occurs when the organism is mechanically disturbed in nature. We thus regard the stiff state seen in the present study as representative of the stiff state occurring naturally in the intact dermis. The stiff state was characterized, in the constant-frequency experiments, by high stiffness, high deformation energy, low dissipation ratio, and low J index. In the constant-maximum-strain experiments, this state was characterized by high moduli and low tan δ. The low values in tan δ and dissipation ratio implied that elasticity prevailed over viscosity. Tan δ was less than 0.1 when the frequency exceeded 0.1 Hz, which implies that the contribution of the viscous component was quite small. This and the low J index imply that the tissue behaved rather like a linear elastic solid at frequencies higher than 0.1 Hz. The high values of stiffness, moduli, and deformation energy are the features associated with the increase in the elastic modulus. Thus, in short, the dermis in the stiff state behaved like a stiff spring. This state has been believed to function in posture maintenance and mechanical defense (Motokawa, 1985). The stiff, spring-like properties seem to be adaptive features for such functions. The high stiffness is helpful in defense and body support, and the springy feature helps restore the original posture after the imposed force is removed. The dominance of elasticity over viscosity also helps by minimizing plastic flow.

Soft state

The soft state is characterized in the constant-frequency experiments by low stiffness, low deformation energy, high dissipation ratio, high J index in unloading, and strain-induced softening. In the constant-maximum-strain experiments, the soft state was characterized by low moduli and high tan δ. Tan δ was about 1 over a wide frequency range, which implies that the contribution of the viscous component was as large as that of the elastic component. At the lowest frequency, tan δ exceeded 1, indicating the dominance of the viscous component. A significant contribution of the viscous component was also found in the constant-frequency experiments that showed a high dissipation ratio in the soft state.

When the maximum strain exceeded a limit strain of about 10%, stiffness decreased as the maximum strain increased. This phenomenon was never observed in other states. Although strain-induced softening has not been reported previously, we could explain the rather contradictory results reported for other sea cucumbers by this strain-induced softening phenomenon. The soft state in the present study was induced by calcium chelation. This procedure was found to cause drastic softening in creep tests (Hayashi and Motokawa, 1986), whereas in dynamic tests it caused much less softening (Szulgit and Shadwick, 2000) or no detectable changes (Shibayama *et al.*, 1994). Although Szulgit and Shadwick (2000) measured shear modulus, not elastic modulus, and thus strict comparison is not possible, the difference in the extent of softening seems to be interpretable, at least in part, by the difference in the strain used. In creep tests, the dermis was usually subjected to fairly large strain, while in dynamic tests, the strain imposed was much smaller than the limit strain of the present sea cucumber. In creep tests, the dermis is very likely in the strain-induced soft state, but in the previous dynamic tests it probably was not in that state.

Strain-induced softening of the dermis was observed in an intact sea cucumber that was subjected to large repetitive deformations (Motokawa, 1988), and thus it seems very likely that the state in CaFASW mimicked the soft state of intact animals. The dermis in CaFASW showed a drastic decrease in stiffness when the deformation exceeded the limit strain. This unique behavior, together with the quite high energy dissipation ratio in the soft state, seems to have adaptive significance in autotomy and fission. Sea cucumbers show evisceration, a kind of autotomy. They contract the body to increase the pressure in the coelomic cavity, causing a rupture in the body wall; they eject their viscera through that hole. Because the dermis in the ruptured portion is very soft to the touch, that part is no doubt in a soft state. The scenario for how the strain-induced softening works in the evisceration process is as follows. The animal would first make a small portion of the dermis—that to be ruptured—soft. At this stage, the softened part still contributes to the integrity of the body wall because the stiffness of the soft state at low strain is not as low as that after having exceeded the limit strain. The animal would then increase the coelomic pressure, causing larger deformations in the softened part. Once the deformation exceeds the limit strain, the stiffness drastically decreases and so the dissipation ratio increases, which allows the dermis to continue deforming at the same pressure (or even under lower pressure) until rupture. This is positive feedback: the more deformed the dermis, the more easily the dermis is deformed. Such mechanical properties allow the animal to eviscerate with only a transient increase in the coelomic pressure, and thus to confine the rupture to the small portion initially softened, leaving the rest of the dermis intact.

Standard state

We employed the convention used in previous studies that the dermis rested in ASW, was taken as the standard state (Motokawa, 1984a). We tested the dermis after a resting period of 1 day in ASW. Such a lengthy resting period was chosen because the dermis, when rested for less than 15 h, showed stiffness values that were between those of the stiff state and the standard state. Thus, recovery from the effects of handling at preparation took quite a long time in this species. The long resting period seems not to adversely affect the dermis, because the sample rested for 1 day showed clear responses both to KASW and to ACh. Previous studies did not employ such a long resting period, which may be one reason for the notoriously large variations in the reported mechanical properties of non-stimulated dermis in ASW (Motokawa, 1984c; Hayashi and Motokawa, 1986; Szulgit and Shadwick, 2000).

By touching the living sea cucumber, we can feel the stiffening of the body wall. If such a stiffened body wall is then vigorously squeezed, it becomes very soft—soft enough to show a viscous flow (Motokawa, 1988). The isolated dermis in the standard state also showed both stiffening and softening responses. Thus it seems reasonable to suppose that the dermis of the intact animal at rest is in a state that corresponds to the present standard state; in this state, the animal is likely to change its body shape for movement. The standard state showed a J-shaped stress-strain relationship with a prominent flat toe region followed by a steep pole region. The toe region allows animals to change their posture easily, with little energy expenditure, by using their body wall muscles. In contrast, to protect the animal from damage, the steep region resists large, externally imposed forces. Thus the standard state with its J-shaped stress-strain curve seems to have adaptive significance.

The standard state showed mechanical properties intermediate between the stiff and soft states, and thus the standard state appears to be just an intermediate between two extremes. Close inspection of the stress-strain relationship, however, suggests that the mechanisms of stiffening and of softening from the standard state are probably different (see next section), and thus we conclude that the dermis of the sea cucumber can assume three distinct mechanical states—stiff, standard, and soft.

Simple polymer model and implications for mechanism of catch

The dermis of the sea cucumber is composed mainly of extracellular materials whose mechanical properties have been thought to determine those of the whole dermis. The main components of the extracellular materials are macromolecules such as collagen and proteoglycans (Matsumura, 1974; Kariya *et al.*, 1990). The dermis shows continuous creep to final breakage under even a small load. This behavior is observed not only in the standard state (Motokawa, 1981) but also in soft and stiff states (unpubl. obs.), which suggests that the main components of the dermis do not make covalent cross-links with each other. It seems to be possible to regard dermis as a blend of non-cross-linked polymers, and thus it is tempting to interpret the present results in terms of polymer science.

Let us suppose that the force-bearing structure in the dermis is a meshwork of polymers. In the meshwork, polymer molecules make a noncovalent bond with adjacent molecules at each crossing point of the molecular mesh. The polymer chain between adjacent crossing points is here called a segment. Two kinds of bonds are postulated in the meshwork. One is the intermolecular bond that forms the crossing point of the meshwork, and the other is the segmental bond found within the molecular chain that comprises the segment (Fig. 9). A part of the molecule in the segment is presumed to take a folded structure in which the folds were maintained by intra-molecular or segmental bonds. Such bonds make the segment less flexible and resistant to stretch. The introduction of inter-molecular bonds implies that more molecules in the dermis are recruited into the force-bearing meshwork.

When the dermis in the standard state is stretched, each molecular segment freely rotates around the crossing points of the mesh until all the segments become parallel to the direction of stretch. Further stretch directly stretches the segment and thus stretches the segmental bonds (central column of Fig. 9). The free rotation of segments corresponds to the toe region of the J curve, and the direct stretching of segments corresponds to the pole region. The unloading curve shows a higher J index than that of the loading curve. This implies that stretching segments induces some plastic deformation. Such plastic deformation must be temporary rather than permanent, because the next hysteresis loop exhibited exactly the same shape. To explain this behavior, we postulate that some segmental bonds are stretched plastically, but they recover their original state in the unloading and compressing phases that follow. Temporarily plastic behavior explains the rather high dissipation ratio seen in the standard state.

Stiffening stimulation induces inter-molecular bonds, which reduces the segment length of the mesh (upper right of Fig. 9). A reduced segment length accounts for the short toe region. It also increases the resistance to rotation around crossing points because a smaller mesh size increases the resistance to displacement of water from the mesh, and thus increases the slope of the toe region. An increase in intermolecular bonds recruits more molecules into the meshwork, and thus increases the resistance to stretch of the meshwork. This explains the higher stiffness of the pole region. The newly recruited molecules are presumed not to contain plastic segmental bonds given the small difference between loading and unloading curves and the low dissipation ratio in the stiff state.

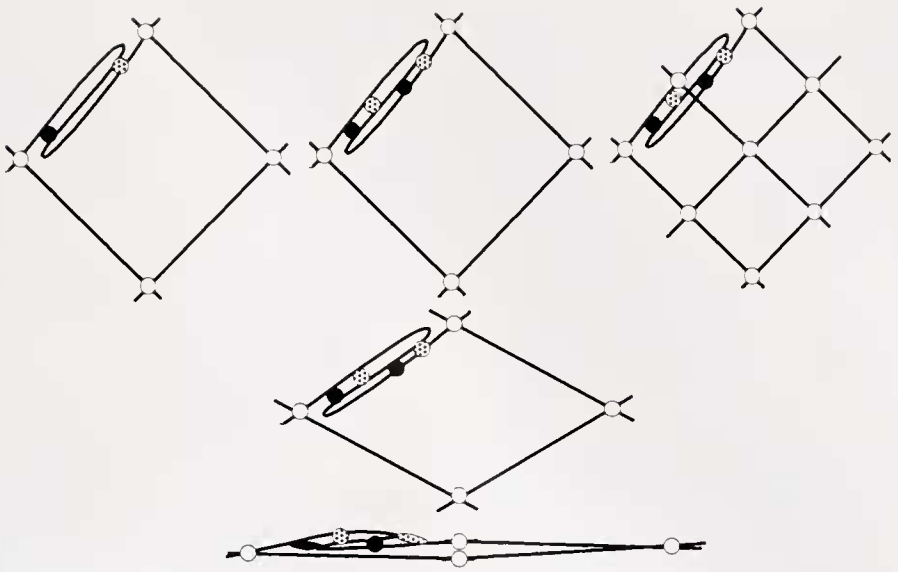

Figure 9. Schematic of a simple polymer model for the dermis. A single mesh is drawn. Top row portrays, from left to right, the soft state, the standard state, and the stiff state. Hollow circle, intermolecular bond; filled circle, segmental bond that deforms elastically when stretched; stippled circle, segmental bond that deforms plastically when stretched. The folded structure of the segment is drawn only for one side of a mesh. Central column is the mesh of the standard state under increasing strain from top to bottom when stretched horizontally. The mesh is free to deform (middle); the segmental bonds experience deformation after the segments become oriented parallel to the direction of stretch (bottom).

In the soft state, the length of the toe region remained the same as that in the standard state. From this result we postulate that the segment length remains the same, and thus the number of inter-molecular bonds remained unchanged at the transition from standard to soft states (upper left of Fig. 9). The segmental bonds are, however, postulated to decrease in number. Removal of segmental bonds makes the segment more flexible and stretchy, which accounts for the low stiffness of the pole region in the soft state. A fair proportion of the remaining segmental bonds show plastic deformation on stretch, producing a fairly large J index at unloading and a large dissipation ratio in the soft state. In the soft state, segmental bonds break when the strain exceeds some limit. This endows the model with strain-softening behavior. The loss of segmental bonds that had held the folded structure of the chain results in elongation of the segment. This explains the longer toe region in samples that experienced strain-induced softening. The breakage of bonds also accounts for the decrease in the maximum stress.

This meshwork model simulates well the mechanical behavior of the dermis with only a small number of assumptions. The model suggests that the molecular mechanism involved in stiffening is different from that involved in softening. Inter-molecular bonds are associated with changes between the standard state and the stiff state, whereas segmental bonds or intra-molecular bonds are associated with changes between the standard state and the soft state. An increase in E' associated with the formation of bonds between molecules has been reported in the collagenous mesogloea of a sea anemone (Gosline, 1971). The stiffening mechanism and the softening mechanism seem to have their own cross-bridging molecules. Tensilin, a protein that stiffens the dermis by binding to collagen (Tipper *et al.*, 2003), is a candidate for the inter-molecular bonding agent. The presence of a softening molecule has also been shown (Koob *et al.*, 1999; Szulgit and Shadwick, 2000). The stiffening mechanism and the softening mechanism also seem to have their own neural pathways (Motokawa, 1987; Birenheide *et al.*, 1998). In the present model, calcium ions are involved in segmental bonds. Calcium ions have a number of possible sites that they affect in both polymer systems and in biological systems. They seem to have some roles in a "polymer system" of the dermis because detergent-treated dermis is quite sensitive to calcium ions (Motokawa, 1994). They are also probably involved in the "biological system" of the dermis, affecting neuronal activities, secretion processes, or both (Motokawa and Hayashi, 1987; Trotter and Koob, 1995). Calcium translocation in the holothurian dermis has been suggested (Matsuno and Motokawa, 1992). Thus calcium ions no doubt play one or more important roles in the mechanism of connective tissue catch.

A meshwork of noncovalently cross-linked polymers gives an E'-frequency curve with four characteristic regions (Ferry, 1980). They are, from the high-frequency end to the low-frequency end, the glass region with a high value of E', the transition region with decreasing E' as frequency decreases, the rubbery or plateau region of constant E', and the flow region of decreasing E' as the frequency decreases.

These four regions are all apparent only when measurements are performed over a very wide range of frequencies, which is often not practicable. In the present study, the dermis in the soft state showed an E'-frequency curve with decreasing E' as frequency decreases in the lowest frequency region. It is reasonable to regard this region as the flow region because a tan δ value of 10 implies that the dermis behaves like a liquid, and because the softened intact dermis does exhibit flow (Motokawa, 1988). The stiff state showed an increase in E' with increasing frequency to reach a constant value of E' of about 5 MPa. Because E' in the glass state is 2 orders of magnitude higher than this (Fukahori, 2000), the high-frequency region of the stiff state is very probably the plateau region, not the glass region.

In polymer science, it is possible to construct a single E'-frequency curve from experimental data of limited frequency ranges by using the time-temperature superposition principle. For linear viscoelastic materials such as amorphous polymers, the effects of time and temperature on mechanical properties are equivalent; thus the curve at one temperature can be superimposed upon those at different temperatures by shifting the curves from lower temperatures to the left and those from higher temperatures to the right along the frequency axis to generate a smooth master curve (Ferry, 1980). This method is convenient because it generates a single curve that gives an overview of the frequency dependence of mechanical properties. A master curve is usually made by varying the temperature. It is, however, sometimes composed from curves derived from different concentrations of polymers or in solutions of different ionic strength (Gibbs *et al.*, 1968). We attempted to generate an "apparent master curve" in order to get a single curve that gives an overview of the frequency dependence of mechanical properties of the holothurian dermis. Temperature manipulation was not practicable because temperature greatly affected the mechanical properties, acting not only directly on the polymer meshwork but also indirectly through affecting the activities of nerves and secretory cells controlling mechanical properties. Instead we shifted the curve in the stiff state to the right and that in the soft state to the left, leaving that of the standard state as a reference. We could construct a smooth curve of E' with four different phases quite similar to the usual master curve of polymers (Fig. 10), although there is no physicochemical theory at hand that supports the present procedure. Therefore, the similarity is just an apparent one. A smooth curve could also be generated on E'' by lateral shifting (data not shown). The fact that we could construct a smooth curve suggests that some physicochemical processes corresponding to frequency shifts occurred at state changes.

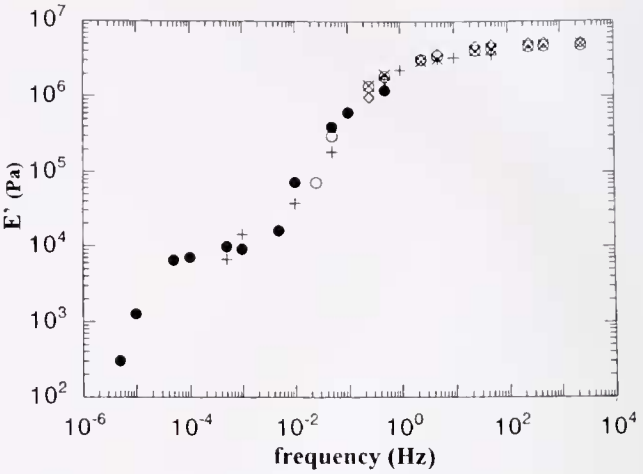

Figure 10. "Apparent master curve" of storage modulus E'. Hollow circle, the stiff state (dissection); hollow diamond, the stiff state (KASW); ×, the stiff state (ACh); +, the standard state; filled circle, the soft state. The logarithm of the shift factor was 1.7 for the stiff states; for the soft state it was −2, meaning that the curve shifted to the left by 2 orders of magnitude in frequency.

Acknowledgments

We thank Drs. Makoto Kaibara and Akio Sakanishi for discussion, and the staff of Sesoko Station, Tropical Biosphere Research Center, University of the Ryukyus, for the supply of sea cucumbers. Supported by Grant-in-aid for scientific research on priority area (A) "Molecular synchronization for design of new materials system."

Literature Cited

Birenheide, R., M. Tamori, T. Motokawa, M. Ohtani, E. Iwakoshi, Y. Muneoka, T. Fujita, H. Minakata, and K. Nomoto. 1998. Peptides controlling stiffness of connective tissue in sea cucumbers. *Biol. Bull.* **194:** 253–259.

Eylers, J. P. 1982. Ion-dependent viscosity of holothurian body wall and its implications for the functional morphology of echinoderms. *J. Exp. Biol.* **99:** 1–8.

Ferry, J. D. 1980. *Viscoelastic Properties of Polymers,* 3rd ed. Wiley, New York. 641 pp.

Fukahori, Y. 2000. *Kobunshi no Rikigaku* (Mechanics of Polymers, in Japanese). Gihodo, Tokyo. 384 pp.

Gibbs, D. A., E. W. Merrill, and K. A. Smith. 1968. Rheology of hyaluronic acid. *Biopolymers* **6:** 777–791.

Gosline, J. M. 1971. Connective tissue mechanics of *Metridium senile.* II. Visco-elastic properties and macromolecular model. *J. Exp. Biol.* **55:** 775–795.

Greenberg, A. R., and J. P. Eylers. 1984. Influence of ionic environment on the stress relaxation behavior of an invertebrate connective tissue. *J. Biomechanics* **17:** 161–166.

Hayashi, Y., and T. Motokawa. 1986. Effects of ionic environment on viscosity of catch connective tissue in holothurian body wall. *J. Exp. Biol.* **125:** 71–84.

Kariya, Y., S. Watabe, K. Hashimoto, and K. Yoshida. 1990. Occurrence of chondroitin sulfate E in glycosaminoglycans isolated from the body wall of sea cucumber *Stichopus japonicus.* *J. Biol. Chem.* **265:** 5081–5085.

Koob, T. J., M. M. Koob-Edmunds, and J. A. Trotter. 1999. Cell-derived stiffening and plasticizing factors in sea cucumber (*Cucumaria frondosa*). *J. Exp. Biol.* **202:** 2291–2301.

Matsumura, T. 1974. Collagen fibrils of the sea cucumber, *Stichopus*

japonicaus: purification and morphological study. *Connective Tissue Res.* **2:** 117–125.

Matsuno, A., and T. Motokawa. 1992. Evidence for calcium translocation in catch connective tissue of the sea cucumber *Stichopus chloronotus. Cell Tissue Res.* **267:** 307–312.

Motokawa, T. 1981. The stiffness change of the holothurian dermis caused by chemical and electrical stimulation. *Comp. Biochem. Physiol.* **70C:** 41–48.

Motokawa, T. 1982. Factors regulating the mechanical properties of holothurian dermis. *J. Exp. Biol.* **99:** 29–41.

Motokawa, T. 1984a. Connective tissue catch in echinoderms. *Biol. Rev.* **59:** 255–270.

Motokawa, T. 1984b. Viscoelasticity of holothurian body wall. *J. Exp. Biol.* **109:** 63–75.

Motokawa, T. 1984c. The viscosity change of the body-wall dermis of the sea cucumber *Stichopus japonicus* caused by mechanical and chemical stimulation. *Comp. Biochem. Physiol.* **77A:** 419–423.

Motokawa, T. 1985. Catch connective tissue: the connective tissue with adjustable mechanical properties. Pp. 69–73 in *Echinodermata,* B. F. Keegan and B. D. S. O'Connor, eds. A. A. Balkema, Rotterdam.

Motokawa, T. 1987. Cholinergic control of the mechanical properties of the catch connective tissue in the holothurian body wall. *Comp. Biochem. Physiol.* **86C:** 333–337.

Motokawa, T. 1988. Catch connective tissue: a key character for echinoderms' success. Pp. 39–54 in *Echinoderm Biology,* R. D. Burke, P. V. Mladenov, P. Lambert, and R. L. Parsley, eds. A. A. Balkema, Rotterdam.

Motokawa, T. 1994. Effects of ionic environment on viscosity of Triton-extracted catch connective tissue of a sea cucumber body wall. *Comp. Biochem. Physiol.* **109B:** 613–622.

Motokawa, T., and Y. Hayashi. 1987. Calcium dependence of viscosity change caused by cations in holothurian catch connective tissue. *Comp. Biochem. Physiol.* **87A:** 579–582.

Oka, S. 1974. *Reorji (Rheology,* in Japanese). Shokabo, Tokyo. 481 pp.

Shibayama, R., T. Kobayashi, H. Wada, H. Ushitani, J. Inoue, T. Kawakami, and H. Sugi. 1994. Stiffness changes of holothurian dermis induced by mechanical vibration. *Zool. Sci.* **11:** 511–515.

Szulgit, G. K., and R. E. Shadwick. 2000. Dynamic mechanical characterization of a mutable collagenous tissue: response of sea cucumber dermis to cell lysis and dermal extracts. *J. Exp. Biol.* **203:** 1539–1550.

Tipper, J. P., G. Lyons-Levy, M. A. L. Atkinson, and A. Trotter. 2003. Purification, characterization and cloning of tensilin, the collagen-fibril binding and tissue-stiffening factor form *Cucumaria frondosa* dermis. *Matrix Biol.* **21:** 625–635.

Trotter, A., and T. J. Koob. 1995. Evidence that calcium-dependent cellular processes are involved in the stiffening response of holothurian dermis and that dermal cells contain an organic stiffening factor. *J. Exp. Biol.* **198:** 1951–1961.

Wainwright, S. A., W. D. Biggs, J. D. Currey, and J. M. Gosline. 1976. *Mechanical Design in Organisms.* Princeton University Press, Princeton. 423 pp.

Wilkie, I. C. 1996. Mutable collagenous tissue: extracellular matrix as mechano-effector. Pp. 61–102 in *Echinoderm Studies,* vol. 5, M. Jangoux and J. M. Lawrence, eds. A. A. Balkema, Rotterdam.

Wilkie, I. C. 2002. Is muscle involved in the mechanical adaptability of echinoderm mutable collagenous tissue? *J. Exp. Biol.* **205:** 159–165.